BNL-65540

CHAPTER NO. 10

MODELS OF SUPEROXIDE DISMUTASES

Diane E. Cabelli*, Dennis Riley,** Jorge A. Rodriguez,***

Joan Selverstone Valentine,*** and Haining Zhu***

*Department of Chemistry, Brookhaven National Laboratory, Upton, NY 11973

** Monsanto Co., 800 N. Lindbergh Blvd., St. Louis, MO 63167

***Department of Chemistry and Biochemistry, UCLA, Los Angeles, CA 90095-1569

CHAPTER NO. 10

MODELS OF SUPEROXIDE DISMUTASES

1. Introduction

1.1 Superoxide dismutases

Superoxide dismutase enzymes catalyze the disproportionation of superoxide to give dioxygen and hydrogen peroxide (1) (equation 1.1).

$$2\,O_2^{\cdot-} + 2\,H^+ \rightarrow O_2 + H_2O_2 \qquad (10.1)$$

Three different, structurally unrelated types of superoxide dismutase (SOD) enzymes have been identified: the copper-zinc SODs, the manganese or iron SODs, and the nickel SODs. The manganese and iron SODs are clearly related to one another based on similarities in their amino acid sequences and their three-dimensional structures.

1.2 Superoxide toxicity and biological function of SODs

Superoxide anion, $O_2^{\cdot-}$, is formed as a normal byproduct of aerobic metabolism from a large number of sources, such as cellular respiration, activated polymorphonuclear leukocytes, endothelial cells, and mitochondrial electron flux; and it has been demonstrated to be a mediator of ischemia-reperfusion injury, inflammatory diseases and vascular diseases (2-4). SOD enzymes are believed to play important roles as antioxidants in accelerating the conversion of superoxide to peroxide, thereby preventing direct reactions of superoxide that may do damage to sensitive targets in the cell (1).

The identities of several individual chemical reactions that contribute to the toxicity of superoxide have been defined. One particularly important type of biological reaction of superoxide is with solvent-exposed iron-sulfur clusters in enzymes such as aconitase. The reaction of superoxide with these centers has been demonstrated to inactivate such enzymes both *in vitro* and *in vivo* and to increase levels of intracellular free reduced iron, which itself can catalyze the oxidative damage of other cellular components by hydrogen peroxide and other oxidants (Fenton-type chemistry) (5). Similarly, it has been shown that superoxide can induce the reductive release of iron from ferritin, the major intracellular iron storage protein (6). The resultant Fenton

DISCLAIMER

chemistry which is unleashed has been proposed to be the source of cardiotoxicity of anthracycline antitumor agents (7).

Recent literature has also documented the high reactivity of the protonated conjugate acid derived from superoxide, perhydroxyl radical, with important biomolecules. This potent oxidizing agent has been shown to be a competent and selective initiator of the autoxidation of lipid membrane components with its site of attack being *only* at the allylic positions in unsaturated fatty acids (8, 9). The products from the resultant highly selective chain autoxidations are leukotrienes (e.g., LTB_4) and prostanoids which are responsible for the upregulation of proinflammatory cytokines (e.g., TNF_a) implicated in autoimmune diseases. The perhydroxyl radical has also been demonstrated to nick DNA under biomimetic conditions and, unlike some other highly reactive oxidants such as hydroxyl radical, with high sequence specificity (10).

Our understanding of the physiological roles of SODs is as yet far from complete. A particularly surprising recent result was the demonstration that mice lacking the gene for CuZnSOD develop relatively normally (11), although fibroblasts from these CuZnSOD-deficient mice are markedly more sensitive to redox cycling drugs than are the wild-type cells (12). By contrast, yeast lacking the gene for CuZnSOD grow poorly in air and die rapidly in stationary phase (13), and both yeast and mice lacking the genes for the mitochondrial MnSOD have drastically reduced life spans (13-15).

Superoxide and other reactive oxygen species have also been shown to function as secondary messengers in signaling pathways in higher organisms (3, 16). Thus, a cell may respond to a stimulus that is not due to changes in oxidative stress by generating reactive oxygen species that diffuse to a target, react, and thereby transduce the signal. Thus the possibility exists that SODs could play roles in signaling pathways in addition to performing their antioxidant functions, suggesting that modulation of the redox state of the cell may provide an explanation for the protective effects against cancer exerted by some antioxidants, as well as why ROS (reactive oxygen species) activate transcription factors such as NFκB (16).

1.4 Synthetic and engineered SODs

Attempts to make synthetic SODs began shortly after the initial discovery of the enzymes, and they continue to this day. However, only recently have investigators succeeded in making complexes that not only have high SOD activity but that also show activity *in vivo* and are potentially suitable for use as drugs (17). Initial studies focused on copper complexes as mimetic compounds for CuZnSOD, but it was quickly realized that synthetic copper complexes usually do not withstand the high

affinities of complexing species that are found *in vivo*, such as bovine serum albumin and the myriad of proteins and amino acids that are found in cells and sera. The copper complexes of stronger binding ligands, such as copper porphyrin or EDTA complexes, have generally been found to be inactive to superoxide radicals (18).

This endeavor has been more successful in the case of manganese complexes as SOD mimics. Two types of manganese-containing synthetic SODs, one with porphyrin ligands (18-20) and the other with a variety of macrocyclic ligands (21-23) have been shown to have significant SOD activity *in vivo*. There has been much less information about the potential of iron and nickel complexes as SODs, although recent studies suggest that SODs based on macrocyclic complexes of iron are feasible (24). A synthetic FeSOD, prepared by reengineering the protein thioredoxin to contain an iron-binding site, has also been reported to have high SOD activity *in vitro* (25).

1.5 Focus of this review

Our knowledge of the mechanistic details of the reaction of superoxide with transition metal complexes has increased significantly in recent years, and dramatic successes have been achieved recently in the development of synthetic SODs with great potential as pharmaceuticals. At the same time, our understanding of the mechanisms of the reactions of the naturally occurring SOD enzymes has also deepened. In this review, we first describe the mechanistic pathways that appear to be operating in reactions of some of the coordination complexes that have been studied as SOD mimics. We then attempt to apply this knowledge in analyzing the enzymatic reactions of the superoxide dismutase enzymes.

2. Superoxide chemistry in aqueous solution

2.1 Background

The physical and chemical behavior of superoxide, $O_2^{\cdot-}$, and its protonated form, the perhydroxyl radical, HO_2, in both aqueous and non-aqueous solutions is described in a two-volume series by Afanas'ev (26), and several reviews covering aspects of HO_2 and $O_2^{\cdot-}$ chemistry in aqueous (27) or non-aqueous (28) chemistry have appeared recently. This section will briefly review the physical properties of superoxide and the perhydroxyl radical in aqueous solution as a background to understanding its reactivity with metal ions and complexes as well as with the superoxide dismutase (SOD) enzymes.

2.2 Physical properties

The equilibrium between HO_2 and its conjugate base, O_2^-, occurs with a pK of 4.8 in aqueous solution (equation 10.2) (29, 30).

(10.2)

$$HO_2 \rightleftharpoons O_2^- + H^+$$

$$K_1 = 1.6 \times 10^{-5}\ M$$

Both oxy-radicals absorb light in the ultraviolet, with maxima at 245 nm and 225 nm for O_2^- and HO_2 respectively. Their extinction coefficients are substantially different: $\epsilon_{245\ nm} = 2350\ M^{-1}cm^{-1}$ for O_2^- and $\epsilon_{225\ nm} = 1400\ M^{-1}cm^{-1}$ for HO_2.

Reduction potentials for O_2, O_2^-, and HO_2 in aqueous solution at versus NHE, with unit concentration used as the standard state for all reactants and products, are $E^0\ (O_2 + e^- \rightarrow O_2^-) = -0.16$ V at pH 7, $E^0\ (O_2 + H^+ + e^- \rightarrow HO_2) = +0.12$ V at pH 0, $E^0\ (O_2^- + 2H^+ + e^- \rightarrow H_2O_2) = +0.89$ V at pH 7, and $E^0\ (HO_2 + H^+ + e^- \rightarrow H_2O_2) = +1.44$ V at pH 0. (The first two E^0 values are shifted by -0.17 V if unit pressure is used for the standard state of dioxygen (O_2). Compilations of thermodynamic parameters for HO_2 and O_2^- under many different conditions are available elsewhere (31, 32).

2.3 Chemical reactivity of superoxide and perhydroxyl radicals

The disproportionation of superoxide and perhydroxyl radicals to yield hydrogen peroxide and dioxygen occurs via a pH dependent mechanism involving reactions 10.3-10.5. Reaction 10.5 does not occur in the pH range of 0.2-13.

$$HO_2 + HO_2 \rightarrow H_2O_2 + O_2 \qquad (10.3)$$

$$k = 8.3 \times 10^5\ M^{-1}s^{-1}$$

$$HO_2 + O_2^- \xrightarrow{H^+} H_2O_2 + O_2 \qquad (10.4)$$

$$k = 9.7 \times 10^7\ M^{-1}s^{-1}$$

$$O_2^- + O_2^- \rightarrow \text{no reaction} \qquad (10.5)$$

The disparity in the rates of these three reactions illustrates two important aspects of superoxide reactivity: (a) Reductions by superoxide are generally faster than reductions by perhydroxyl (compare reactions 10.3 and 10.4). (b) Perhydroxyl is capable of fast one-electron oxidation of substrates while superoxide anion usually is not (compare reactions 10.4 and 10.5). Those exceptional cases in which superoxide is observed to oxidize substrates rapidly occur only when a proton is available to transfer to the O_2^- moiety simultaneously with acceptance of an electron, i.e., proton-coupled electron transfer, resulting in formation of hydroperoxide anion, HO_2^- (reaction 10.6) rather than simple electron transfer to give peroxide dianion, O_2^{2-}.

$$X \cdots O_2^- \cdots H\text{-}Y \rightarrow X^+ + HO_2^- + Y^- \qquad (10.6)$$

An example of a fast oxidation by superoxide in which proton-coupled electron transfer to superoxide is likely to be occurring is the rapid oxidation of hydroquinones by superoxide (33) (reaction 10.7).

$$k = 1.7 \times 10^7\ M^{-1}s^{-1} \qquad (10.7)$$

Alternatively, a metal ion may be oxidized by superoxide in an oxidative addition reaction to give a metal peroxo complex, where the peroxide is stabilized by coordination to the metal ion rather than by protonation, followed by peroxide dissociation, resulting in overall oxidation of the metal ion. In this case, the electron transfer to form a metal-bound peroxide can precede the protonation step because the metal ion stabilizes the O_2^{2-} ligand as it is formed (reaction 10.8).

$$M^{n+} + O_2^- \rightarrow M^{(n+1)+}(OO^{2-}) \xrightarrow{H^+} M^{(n+1)+} + H_2O_2 \qquad (10.8)$$

3. Mechanism of the superoxide dismutase reaction

3.1 The superoxide dismutase reaction

Superoxide dismutases are catalysts of the superoxide disproportionation reaction (equation 10.1). The superoxide dismutase enzymes known to date are relatively small metalloproteins containing either Cu and Zn, Mn, Fe, or Ni. The ubiquitous presence

of these enzymes in living organisms has led to great interest in the mechanism by which these enzymes so efficiently catalyze reaction 10.1 and in the synthesis of model compounds that will function as efficiently as the enzymes.

The superoxide dismutase mechanisms that are known may be conveniently divided into two separate steps, the first involving reduction by superoxide to afford dioxygen and the second involving oxidation by superoxide yielding hydrogen peroxide. In the following discussion, these two steps are discussed and analyzed separately.

3.2 Reduction by superoxide to give dioxygen

The most characteristic reaction of superoxide is as a one-electron reducing agent, and many examples are known of relatively fast reactions of this type. Two general mechanistic pathways involving redox changes at a metal center should be considered (reaction 10.9): coordination (inner-sphere) of superoxide followed by electron transfer to a metal ion and outer-sphere electron transfer to a metal ion without prior coordination of superoxide.

(10.9)

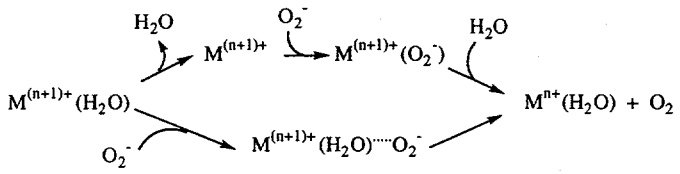

Variants of these reactions are reactions in which the starting complex is a metal peroxo complex and hydrogen peroxide is released as the metal ion is reduced (reaction 10.10; see reaction 10.44 below for an example).

(10.10)

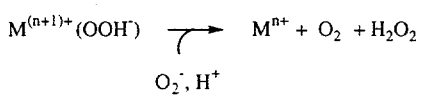

Another possible mechanistic pathway in which superoxide might act as a reducing agent in SOD reactions is via reduction of a metal-bound superoxide affording a metal bound peroxide without change of oxidation state of the metal ion (34) (reaction 10.11).

$$M^{(n+1)+}(O_2^-) + O_2^- \rightarrow M^{(n+1)+}(O_2^{2-}) + O_2 \qquad (10.11)$$

3.3 Oxidation by superoxide to give hydrogen peroxide

As discussed in section 2.3 above, superoxide is observed to be reduced rapidly by substrates to the peroxide level only when proton-coupled electron transfer can occur, i.e., when a proton transfers to the O_2^- moiety simultaneously with transfer of an electron (reaction 10.6). For the case where the reducing agent is a redox metal center, proton-coupled electron transfer to superoxide could conceivably occur with superoxide in the first coordination sphere of the metal ion (reaction 10.12). Such an inner-sphere pathway requires a vacant coordination site on the metal. So it is probable that such a pathway is limited to the rate at which ligand exchange occurs on the metal ion.

(10.12)

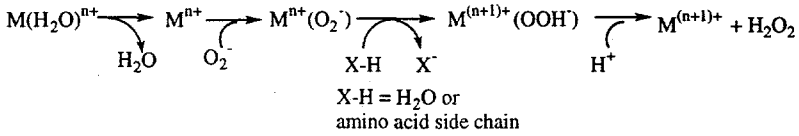

Two different types of outer sphere mechanisms are also possible. Such mechanistic pathways might be advantageous since they could bypass formation of stable metal hydroperoxide complexes, $M^{(n+1)+}(OOH^-)$, whose rates of dissociation could slow down SOD reactions. The first of these outer sphere mechanisms would require that superoxide be hydrogen bonded to two proton donors and not be bonded to the metal ion prior to electron transfer (reaction 10.13). In the case of synthetic SOD mimics, it is difficult to imagine avoiding superoxide complexation as well as achieving the required hydrogen bonding configuration prior to electron transfer, but it is nevertheless a feasible mechanism for SOD enzymes. This mechanism is proposed as a possible mechanism for CuZnSOD in section 5.1.3.3 below.

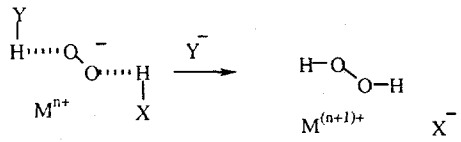

(10.13)

The second outer sphere mechanism involves a coordinated water molecule which is the hydrogen atom donor for a proton-coupled electron transfer (reaction 10.14).

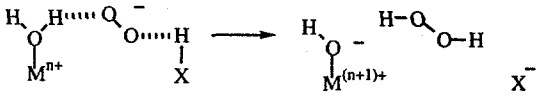

(10.14)

Such a mechanism is reminiscent of the proton-coupled electron transfer pathway postulated for the self-exchange reaction for $Fe(H_2O)_6^{2+/3+}$, i.e., hydrogen atom transfer from $[Fe^{II}(H_2O)_6]^{2+}$ to $[Fe^{III}(H_2O)_5(OH)]^{2+}$ (reaction 10.15) (35, 36).

(10.15)

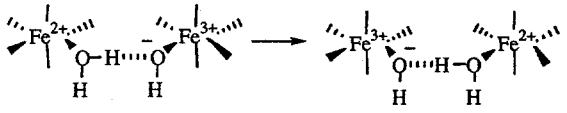

Reaction 10.14 probably cannot occur at a fast rate if the proton donor H-X is not present and oriented correctly for proton transfer simultaneous with electron transfer. In such cases, a pH-dependent pathway may be observed in which the oxidant is actually HO_2 (reaction 10.16). Such a pathway also would fulfill a very important criteria for fast electron transfer; namely, that charge separation cannot develop in the transition state for the electron transfer step if the process is to possess extremely fast rates; i.e., near the diffusion limit, as is observed with SOD enzymes.

(10.16)

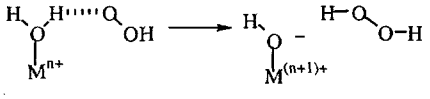

4. Reactions of superoxide with copper, manganese, and iron ions and low molecular weight complexes

4.1 Copper

4.1.1 Aqueous copper ions

The search for low molecular weight copper complexes as model complexes for CuZnSOD has historically received the most attention, in large part due to the high

prevalence of CuZnSOD *in vivo* and the fact that it was the first SOD identified. The reactions of copper ions and many small copper complexes with superoxide have consequently been studied in great detail using pulse radiolysis techniques.

Cupric ions (Cu^{2+}) are reduced by superoxide and by perhydroxyl in aqueous solution with rate constants that are very large: $k_{17} = 10^{10}\ M^{-1}s^{-1}$ and $k_{18} = 10^{9}\ M^{-1}s^{-1}$ (37).

$$O_2^{\cdot} + Cu^{2+} \rightarrow Cu^{+} + O_2 \qquad (10.17)$$

$$HO_2 + Cu^{2+} \rightarrow Cu^{+} + O_2 + H^{+} \qquad (10.18)$$

Reoxidation of the formed cuprous ion (Cu^{+}) by superoxide or perhydroxyl occurs with somewhat slower rate constants: $k_{19} = (5\text{-}8) \times 10^{9}\ M^{-1}s^{-1}$ and $k_{20} = 10^{8}\ M^{-1}s^{-1}$ (37).

$$O_2^{\cdot} + Cu^{+} \xrightarrow{2\,H^{+}} Cu^{2+} + H_2O_2 \qquad (10.19)$$

$$HO_2 + Cu^{+} \xrightarrow{H^{+}} Cu^{2+} + H_2O_2 \qquad (10.20)$$

The high rate constant for reaction 10.19 may suggest that the reaction proceeds by proton-coupled electron transfer as in reaction 10.14 where $HX = H_2O$. An inner-sphere pathway for this reaction is also consistent with the known very fast ($> 10^{9}$) water exchange rates on the aquo copper(II) ion which arise because Cu^{2+} is a Jahn-Teller d^{9} spin system.

As the catalytic process is limited by the slowest rate constant in the cycle, it is clear that at physiological pH (pH = 7.4), the catalytic process involves predominantly $O_2^{\cdot}$ (reactions 10.17 and 10.19) and is very rapid. The limiting feature in this system is that copper hydroxides form as the pH is increased and the insolubility of these copper hydroxides in water limits the observed rate at higher pH.

The rate constants for reactions of superoxide with cuprous or cupric ion are so large at ambient pH that contamination by free copper ions can be a significant problem in determining $O_2^{\cdot}$ lifetime or reactivity in aqueous solution (38). The use of copper chelators can obviate this problem because, as discussed below, the rate constants and reaction mechanisms for copper ions change markedly when they are incorporated in a coordination complex or metalloenzyme.

4.1.2 Copper amino acid and other coordination complexes

The original studies of the reactions of superoxide with copper amino acid complexes demonstrated that the reactions occur with quite large rate constants, but these studies were carried out at a single pH or over a narrow pH range (39-41). Subsequent studies

over a wide pH range were carried out for Cu(II) histidine complexes (42) and Cu(II) arginine complexes (43) which established that, at least in these two systems, the large rate constants occur over the narrow pH range in which the copper(II) amino acid complex had either an open coordination site or an exchangeable water. This observation suggests that the reaction occurs via an inner sphere mechanism, as in reaction 10.9 above. In the case of Cu(II) arginine complexes, the formation of a transient copper(II) superoxo complex was detected in pulse radiolysis experiments (reaction 10.21).

$$[Cu(II)ArgH_2]^+ + O_2^- \rightarrow [Cu(II)(ArgH_2^+)(O_2^-)] \rightarrow Cu(I)\text{-Arginine} + O_2 \qquad (10.21)$$

A particularly interesting series of copper complexes whose reactions with superoxide were studied contain 1,10-phenanthroline or substituted 1,10-phenanthrolines as ligands. The reaction of such complexes with superoxide, hydrogen peroxide, and dioxygen holds particular interest because the copper bis-phenanthroline complexes are known to cleave DNA in the presence of hydrogen peroxide (44-47). This reaction is probably the result of a site specific Fenton-type reaction of $Cu(phen)_2^+$ with H_2O_2. (Reaction 10.22 is the generalized description of this reaction.)

(10.22)

$$LCu(I) + H_2O_2 \longrightarrow \begin{cases} LCu(II)(HO\cdot) + OH^- \\ LCu(II)(OH^-) + HO\cdot \\ Cu(III)L + 2\,OH^- \end{cases}$$

All that is needed to make a catalytic cycle of the $Cu(phen)_2^{2+}$ plus H_2O_2 DNA-cleavage system is the presence of a reductant; e.g., superoxide anion. The rate constants for reactions such as reaction 22 are not fast (see Table 1), but the facile and efficient binding of $Cu(phen)_2^{2+}$ to DNA ensures a high rate of reaction of the oxidant produced in reaction 10.22 with DNA.

The overall mechanism for the reaction of $Cu(phen)_2^{2+}$ (47, 48) with O_2^- proceeds via the formation of a transient copper(II)-superoxo complex (reactions 10.23-10.26).

$$Cu(II)(phen)_2^{2+} + O_2^- \rightarrow Cu(I)(phen)_2^+ + O_2 \qquad (10.23)$$

$$Cu(I)(phen)_2^+ + O_2^- \xrightarrow{2\,H^+} Cu(II)(phen)_2^{2+} + H_2O \qquad (10.24)$$

$$Cu(I)(phen)_2^+ + O_2 \rightarrow [Cu(II)(phen)_2(O_2^-)] \qquad (10.25)$$

$$[Cu(II)(phen)_2(O_2^-)]^+ + Cu(I)(phen)_2^+ \xrightarrow{2\,H^+} 2\,Cu(II)(phen)_2^{2+} + H_2O_2 \qquad (10.26)$$

Table 10.1: Rate Constants for oxidation of various copper(I) complexes by O_2^-, O_2 or H_2O_2 (pH = 7.0, unless specified)

Complex	O_2^-	O_2	H_2O_2
Cu^+_{aq}	10^{10} [a]	$4.6x10^5$ [b]	$4.7x10^3$ [c]
Cu(4,11-dieneN4)$^+$ [d]	--	2.6×10^7	–
$Cu(bpy)_2^+$ [e]	1.8×10^8	5.8×10^4	1.5×10^3
$Cu(phen)_2^+$ [f]	3.0×10^8	5.0×10^4	9.4×10^2
$Cu(5\text{-}Clphen)_2^+$ [g]	2.1×10^8	5.0×10^3	–
$Cu(5\text{-}NO_2phen)_2^+$ [h]	8.3×10^8	5.8×10^2	4.4×10^2
$Cu(5\text{-}Mephen)_2^+$ [i]	2.3×10^8	6.6×10^4	1.6×10^3
$Cu(2,9\text{-}Me_2phen)_2^+$ [j]	2.4×10^8	--	–
CuZnSOD[k]	2×10^9	very slow	0.04

[a] pH = 3-6.5 (49)
[b] pH = 2.1(50)
[c] pH = 2.3 (51)
[d] (52) Cu(4,11-dieneN4)$^+$ = 5,7,7,12,14,14-hexamethyl-1,2,8,11-tetraazocyclotetradeca-4,11-dienecopper(I)
[e] (53) $Cu(bpy)_2^+$ = bis(2,2'-bipyridine)copper(I)
[f] (54) $Cu(phen)_2^+$ = bis(1,10-phenanthroline)copper(I)
[g] (53) $Cu(5\text{-}Clphen)_2^+$ = bis(5-chloro-1,10-phenanthroline)copper(I)
[h] (53) $Cu(5\text{-}NO_2phen)_2^+$ = bis(5-nitro-1,10-phenanthroline)copper(I)
[I] (53) $Cu(5\text{-}Mephen)_2^+$ = bis(5-methyl-1,10-phenanthroline)copper(I)
[j] (53) $Cu(2,9\text{-}Me_2phen)_2^+$ = bis(2,9-dimethyl-1,10-phenanthroline)copper(I)
[k] (55)

4.2. Manganese

4.2.1 Manganese ions and complexes

Reactions of manganese ions and complexes with superoxide are complicated by the simultaneous occurrence of inner and outer sphere pathways for oxidation of manganese(II). Understanding these reactions in detail in important since similar mechanistic pathways are likely to be occurring in reactions of MnSOD with superoxide.

Manganous ion is only soluble and stable at low to neutral pH, and the manganic ion is only stable to disproportionation in acidic solution. In contrast, upon complexation, manganese(II) can be studied over a broad pH range. Pulse radiolysis studies have demonstrated that both Mn^{2+} ions and manganese(II) polyaminocarboxylate complexes react with superoxide to give transient manganous superoxide complexes (56-63) (reactions 10.27-10.29).

$$LMn(II) + O_2^- \rightleftharpoons LMn(II)(O_2^-) \quad (10.27)$$

$$LMn(II)(O_2^-) \xrightarrow{2\,H^+} LMn(III) + H_2O_2 \quad (10.28)$$

$$LMn(II)(O_2^-) + O_2^- \xrightarrow{2\,H^+} LMn(II) + O_2 + H_2O_2 \quad (10.29)$$

The protonated adduct, $LMn(HO_2)$, which could be either $LMn(II)(HO_2)$ or $LMn(III)(HO_2^-)$, is formed at low pH, either by protonation of $LMn(II)(O_2^-)$ (reaction 10.30) or by direct reaction of HO_2 with LMn(II) (reaction 10.31). The mechanism by which the protonated adduct disappears can involve the formation of a bridged binuclear adduct, leading to the formation of LMn(III) (reactions 10.26-10.28). A recent publication (64) suggests that the binuclear adduct is not necessarily formed with manganous ions at low pH. (It should be noted that the species $LMn(III)(HO_2^-)$ is written here as a Mn(III) complex of the hydroperoxide anion HO_2^-, but it could instead be $LMn(II)(HO_2)$, a Mn(II) complex of the perhydroxy radical HO_2.)

$$LMn(II)(O_2^-) + H+ \rightleftharpoons LMn(III)(HO_2^-) \quad (10.30)$$

$$LMn(II) + HO_2 \rightarrow LMn(III)(HO_2^-) \quad (10.31)$$

$$LMn(III)(HO_2^-) + LMn(II) \rightleftharpoons [LMn(III)(HO_2^-)Mn(II)L] \quad (10.32)$$

$$[LMn(III)(HO_2^-)Mn(II)L] \rightarrow LMn(III) + LMn(II) + HO_2^- \quad (10.33)$$

$$LMn(III)(HO_2^-) \rightarrow LMn(III) + HO_2^- \quad (10.34)$$

Protonation of the transient intermediate $LMn(II)(O_2^-)$ to yield peroxide has been observed to be very ligand sensitive. For example, the rate of formation of the Mn(III) complex of pyrophosphate ($P_2O_7^{4-}$) has been shown to be concomitant with the rate of disappearance of O_2^-; no $Mn(II)(O_2^-)$ adduct was observed. An inner sphere mechanism with adduct formation is not precluded in that reaction, but it is clearly impossible to accelerate the formation of the adduct sufficiently for it ever to have an observable lifetime. In contrast, for a manganese(II) complex of TTHA (65) (TTHA = triethylenehexaaminehexaacetate), release of free peroxide occurred via reaction of the Mn(II) superoxo complex with a proton and not water such that, at alkaline pH, the $Mn(II)(O_2^-)$TTHA complex disappeared by a second-order process that can be attributed to dissociation of superoxide (reverse of equilibrium 10.35) followed by spontaneous dismutation of O_2^- via reaction 10.1.

$$LMn(III) + O_2^- \rightleftharpoons L\,Mn(II) + O_2 \quad (10.35)$$

In addition to the facile oxidation of Mn(II) by superoxide, a superoxide dismutase catalytic cycle also, of course, requires the rapid reduction of Mn(III) by O_2^- (the forward step of the equilibrium in reaction 35). Rate constants for this reaction are not easily measured because manganic complexes are generally not very stable at ambient pH. An interesting example of such a determination is described in a pulse radiolysis study of reactions of superoxide with manganese complexes of EDDA (EDDA = ethylenediaminediacetate) (63). The oxidation of Mn(II)EDDA by O_2^- (reactions 10.36 and 10.37) again proceeded via a transient adduct (reaction 10.36), as has been seen for several complexes. In this system, however, it was also possible to form significant concentrations of Mn(III)EDDA by reaction of Mn(II)EDDA with a large burst of O_2^-. The subsequent reduction (reactions 10.38 and 10.39) of Mn(III)EDDA by superoxide could then be observed using a second, smaller burst of O_2^- and was found to display saturation kinetics, suggesting a mechanism that includes formation of a $Mn(III)(O_2^-)$ transient adduct (reaction 10.38). This experiment was only possible because reaction 10.37 was sufficiently fast at neutral pH to allow the rapid formation of Mn(III)EDDA and because equilibrium 10.38 and reaction 10.39 were sufficiently slow relative to reaction 10.37. This system is clearly not an effective biomimetic catalyst for MnSOD because of these slow rates.

$$Mn(II)EDDA + O_2^- \rightarrow Mn(II)EDDA(O_2^-) \quad (10.36)$$

$$Mn(II)EDDA(O_2^-) + H_2O \xrightarrow{H^+} Mn(III)EDDA + H_2O_2 + OH^- \quad (10.37)$$

$$Mn(III)EDDA + O_2^- \rightleftharpoons Mn(III)EDDA(O_2^-) \quad (10.38)$$

$$Mn(III)EDDA(O_2^-) \rightarrow Mn(II)EDDA + O_2 \quad (10.39)$$

It should be noted that the rate constants for reduction of model Mn(III) complexes by O_2^- given in Table 2 are significantly lower than those measured for MnSOD. The reduction of Mn(III)SOD by O_2^- to yield Mn(II)SOD and O_2 is virtually diffusion controlled (ca. 10^9 $M^{-1}s^{-1}$) with no detectable formation of a transient adduct (see section 5.2 below).

The dismutation of O_2^- by various Mn(II)-containing model complexes is generally slow (k_{cat} ca. 10^6-10^7 $M^{-1}s^{-1}$) relative to the enzyme. This catalysis is often limited by reduction of Mn(III) by O_2^-; oxidation of the Mn(II) complexes by superoxide is usually fast (see Table 2). This pattern is also seen with manganous and manganic porphyrins. Oxidation of Mn(II) porphyrins (k ca. 1^{08}-10^{10} $M^{-1}s^{-1}$) and reduction of Mn(III) porphyrins (k ca. 1^{05}-10^8 $M^{-1}s^{-1}$) by O_2^- have been shown to occur via outer-sphere mechanisms (20). The latter rate constants are the ones that control the catalytic efficiency of manganese porphyrins as SOD mimics.

A number of more effective MnSOD synthetic mimics have been synthesized and studied recently. These include the Mn(III)desferrioxamine B green complex (66-69), Mn(II)salen complexes (70), and Mn(II) pentaazamacrocycle complexes (17, 21, 22).

Table 2. Rate Constants for reactions of Mn(II) and Mn(III) complexes with superoxide

Ligand	k(LMn(II) + O_2^-), $M^{-1}s^{-1}$ (pH) (ref.)	k(LMn(III) + O_2^-), $M^{-1}s^{-1}$ (pH) (ref.)
NTA[a]	4×10^8 (4.5) (61) 1.2×10^8 (5.5) (61)	1.2×10^7 (6.0) (59)
EDTA[b]	3×10^7 (4.5) (61) 7.5×10^6 (5.5) (61)	5×10^4 (10.0) (62)
CyDTA[c]	–	7.2×10^5 (9.2) (62)
TTHA[d]	1.75×10^5 (6-8.3) (65)	
$P_2O_7^{4-}$ [e]	2.6×10^7 (6.5) (57) 1.3×10^7 (7.3) (71)	
Formate	4.6×10^7 (4-7) (57)	
Sulfate	5.4×10^7 (2.8-5.6) (57)	
Phosphate	5×10^7 (2-6) (58)	
EDDA[f]	3×10^7 (7.1) (63)	
DFB[g]	3×10^6 (66)	1×10^6 (66)
TMPyP[h]	$(2.5\text{-}3.3) \times 10^9$ (6.7-9.3) (20)	$(3.5\text{-}5.1) \times 10^7$ (5.6-9.3)(20, 72)
TAPP[i]	$(5.6\text{-}20) \times 10^8$ (6.7-9.3) (20)	$(1.5\text{-}13) \times 10^6$ (5.6-9.3) (20, 72)
PFP[j]	$(5\text{-}9) \times 10^9$ (6.7-9.3) (20)	1.7×10^7 (6.7) (20) 4.0×10^5 (9.3) (20)
MnSOD[k]	1.5×10^9 (9.3) (72)	1.5×10^9 (9.3) (72)

[a]NTA = nitriloacetate
[b]EDTA = ethylenediaminetetraacetate
[c]CyDTA = diaminecyclohexane-N,N,N',N'-tetraacetate
[d]TTHA = triethylenetetraaminehexaacetate
[e]$P_2O_7^{4-}$ = pyrophosphate
[f]EDDA = ethylenediaminediacetate
[g]DFB = desferrioxamine B
[h]TMPyP = tetrakis(4-N-methylpyridyl)porphine
[i]TAPP = tetrakis-4-(N,N,N,-trimethylamino)phenylporphine
[j]PFP = tetrakis(N-methylisonicotinomidophenyl)porphine
[k]from *Thermus thermophilus*

Kinetic studies of the reactions of superoxide with a large series of pentaazamacrocyclic complexes of manganese using stopped flow techniques have been particularly informative concerning the details of the mechanistic pathways involved, especially with regard to the role of protons in determining the relative rates of reduction of superoxide when it is bound to a metal ion during catalysis (22).

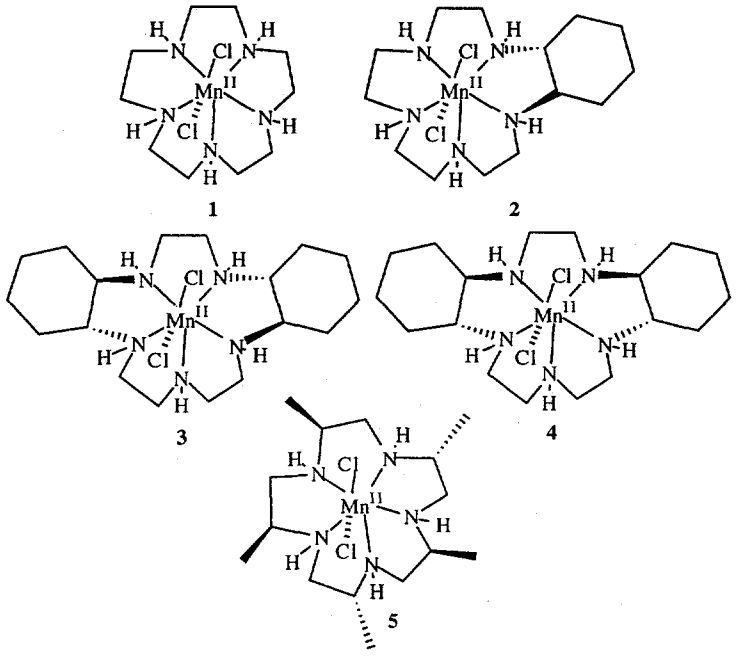

For each of the complexes **1-5**, the catalytic rate of disproportionation of superoxide, k_{cat}, was found to be first order in $[O_2^-]$ and [Mn complex] added. For **1-4**, a plot of the observed k_{cat} at a given pH versus the proton concentration gives a straight line with a non-zero intercept. Thus both a pH dependent and a pH independent pathway were observed. In the case of **5**, by contrast, the rate is pH independent.

The observed rate law is given in equation 10.40.

$$-d[O_2^-]/dt = k_{cat}\,[\text{Mn complex}]\,[O_2^-] = [\text{Mn complex}]\,[O_2^-]\,\{2k_1/K_a[H^+] + 2k_2\} \qquad (10.40)$$

where K_a is the acidity constant for HO_2 ($K_a = 2.04 \times 10^{-5}$). These results are consistent with the following mechanism (reactions 10.41-10.44).

$$LMn(II)(OH_2) + HO_2 \xrightarrow{k_{41}} LMn(III)(OH^-) + H_2O_2 \qquad (10.41)$$

$$LMn(II)(H_2O) + O_2^- \xrightarrow{k_{42}} LMn(III)(OO^{2-}) + H_2O \text{ (inner sphere)} \qquad (10.42)$$

$$LMn(III)(OO^{2-}) + H^+ \xrightarrow{\text{fast}} LMn(III)(OOH^-) \qquad (10.43)$$

$$LMn(III)(OOH^-) + O_2^- + H^+ \xrightarrow{\text{fast}} LMn(II) + H_2O_2 \qquad (10.44)$$

Several interesting comparisons can be made between catalysts **1-5**. Comparison of the k_{cat} observed for the two bis (*trans*-fused) cyclohexano derivatives, **3** and **4**, is particularly interesting (see Table 3). Cyclic voltammetry of **3** and **4** showed identical behavior, with a well-defined reversible one-electron oxidation at $E_{1/2}$ at 0.74 V vs. SHE in anhydrous methanol (22). Nevertheless, their ability to function as SOD catalysts is strikingly different. Complex **3** was found to function at a rate equivalent to native mitochondrial MnSOD at pH = 7.4, while complex **4** exhibited no detectable SOD activity. This striking difference in the catalytic rates of superoxide dismutation for these two steroisomeric complexes is indicative of a powerful influence of the ligand substituents on the rates of reaction with superoxide.

Table 3. Representative values for the proton-dependent and proton independent catalytic rate constants for SOD activity of Mn complexes 1-5 measured over the pH range 7.4-8.3

Complex	k_{41}, $10^{10} M^{-1}s^{-1}$	k_{42}, $10^{7} s^{-1}$	k_{cat} x 10^{-7} $M^{-1}s^{-1}$ (pH = 7.4)
1	0.29	0.91	
2	0.78	1.44	
3	2.25 (1.07 in D_2O)	1.58 (1.83 in D_2O)	12.1
4	0	0	0
5	0	1.91 (1.01 in D_2O)	3.82

Studying the kinetics of the SOD reaction for **3** and **5** in D_2O provided further insight into the details of the rate-limiting electron-transfer steps. Complex **5** exhibits no $[H^+]$ dependence in its SOD activity. The catalytic rates for **3** and **5** in D_2O exhibited kinetic behavior similar to that observed in H_2O. The pH independent rate constant k_2 for **5** was decreased ~45%. For **3**, k_1 decreased by ~50%, but k_2 increased by ~10% (see Table 3).These results, combined with the observations that **4** is not a catalyst, that **5** has no pH dependent component to its k_{cat}, and that k_1 for **1**, **2**, and **3** are approaching diffusion controlled limits, has led to some important conclusions about the mechanism.

The observation that k_2, the rate constant for the pH-independent pathway, is approximately 10^7 $M^{-1}s^{-1}$ for each of these complexes suggests that a dissociative process may be rate-limiting since the rate of loss of water from the inner-coordination sphere of aquo Mn(II) is 0.8 x 10^7 s^{-1}. The modest deuterium isotope effect for k_2 for both **3** and **5**, suggest that this is indeed the case. Rates of solvent exchange on metal ions can be both faster and slower in D_2O than in H_2O, but the fact that there is an effect strongly implies that aquo ligand exchange is involved in the rate-determining step.

Another conclusion that can be drawn from the kinetic experiments is that the near diffusion-controlled rate constant k_1 for the pH dependent electron-transfer

process requires that the barrier to electron transfer to HO_2 be very small. Thus we can conclude that little charge separation develops in the transition state and that the Mn(III) product complex has a structure very similar to the starting Mn(II) complexes so that the reorganization energy is low. The pH dependence on the rate in D_2O supports these conclusions. The decrease in rate for **3** in D_2O resembles that seen for the Fe^{2+}/Fe^{3+} self-exchange reaction in water which is believed to occur via a hydrogen atom transfer from a bound water on Fe(II) (reaction 10.15) (35, 36).

Recent studies provide support for proton-coupled electron transfer as an important pathway for fast electron transfer in biological systems, as suggested recently for photosystem II (73) thereby avoiding the build up of charge separation in the transition state for electron transfer. Additionally, a recent report indicates that the thermodynamics of an H-atom transfer from a Mn-bound water to HO_2 will be favorable; i.e., the bond dissociation energy of an O-H bond of water bound to a Mn(III)(Salen) derivative is 86 kcal/mol. Thus H-atom transfer to HO_2 is energetically allowed since the bond dissociation energy of the O-H bond of hydrogen peroxide is reported to be 87.2 kcal/mol (74).

The ability of **1**, **2**, and **3** (but not **4**) to adopt pseudo-octahedral conformations by folding the macrocyclic ring so that one of the secondary amines occupies an axial site also provides a logical explanation for the dramatic loss of SOD reactivity in the case of **4**. Thus, if the macrocyclic [15]aneN$_5$ ligand possesses C-substituents which, due to intramolecular steric repulsions and angle strains, enable the ligand readily to adopt a folded pseudo-octahedral geometry about the spherically symmetrical Mn(II) ion, as is the case for **1**, **2**, and **3**, then the Mn(II) complex would be poised to undergo facile electron-transfer. Thus the outer-sphere path is expected to proceed through an intermediate pseudo-octahedral $[LMn(II)(H_2O)]^{2+}$ complex with a folded macrocyclic ligand (reaction 10.45), while the inner-sphere substitution pathway would involve a superoxo $[LMn(II)\ (O_2^-)]^+$ six-coordinate intermediate complex, containing the folded macrocyclic ligand, which would be protonated to generate the $[Mn(III)(L)(HO_2)]^{2+}$ pseudo-octahedral complex (reaction 10.46).

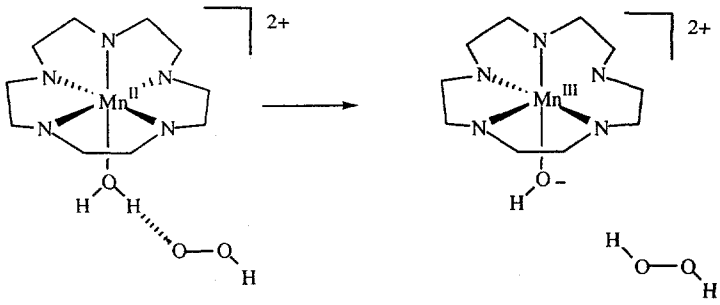

(10.45)

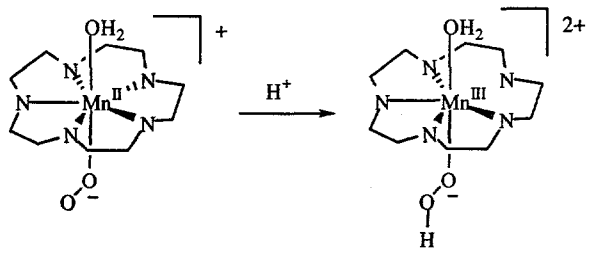

(10.46)

This need to fold the ligand into a conformation that will stabilize a pseudo-octahedral geometry on Mn(II) may be the reason why **5** shows no rate for this pH dependent pathway. Thus the presence of a methyl substituent symmetrically positioned on one carbon of each chelate ring may inhibit folding and thereby block this pathway for fast electron-transfer to HO_2.

4.3. Iron

The aquo-iron system is not an effective superoxide dismutase, as evidenced by the rate constants for the individual reactions in the overall mechanism (75-77) (reactions 10.47-10.50):

$$Fe^{2+} + HO_2 \rightarrow Fe^{3+} + HO_2^- \qquad k_{47} = 1.2 \times 10^6\ M^{-1}s^{-1} \qquad (10.47)$$

$$Fe^{2+} + O_2^- \rightarrow Fe^{3+} + HO_2^- \qquad k_{48} = 1 \times 10^7\ M^{-1}s^{-1} \qquad (10.48)$$

$$Fe^{3+} + HO_2 \rightarrow Fe^{2+} + H^+ + O_2 \qquad k_{49} < 10^3\ M^{-1}s^{-1} \qquad (10.49)$$

$$Fe^{3+} + O_2^- \rightarrow Fe^{2+} + O_2 \qquad k_{50} = 1.5 \times 10^8\ M^{-1}s^{-1} \qquad (10.50)$$

The kinetic values are relatively independent of formate and sulfate, which complex only weakly to iron at low pH. The oxidation of Fe^{2+} by HO_2 occurs by a multistep process at low pH (reactions 10.51-10.54) that is analogous to that described in reactions 10.31-10.34 in the manganese system (78-80).

$$Fe^{2+} + HO_2 \rightarrow Fe^{3+}(HO_2^-) \qquad (10.51)$$

$$Fe^{3+}(HO_2^-) + Fe^{2+} \rightleftharpoons [Fe^{3+}(HO_2^-)Fe^{2+}] \quad (10.52)$$

$$Fe^{3+}(HO_2^-) \rightarrow Fe^{3+} + HO_2^- \quad (10.53)$$

$$[Fe^{3+}(HO_2^-)Fe^{2+}] \rightarrow Fe^{3+} + HO_2^- + Fe^{2+} \quad (10.54)$$

A number of synthetic iron complexes have been reported to catalyze the dismutation of superoxide to oxygen and hydrogen peroxide, although far fewer examples exist than for either copper or manganese. The earliest of these is the $Fe^{III}(EDTA)(H_2O)$ complex (81). While this complex is a poor catalyst with catalytic rate $<10^6 M^{-1} s^{-1}$, the mechanism is nevertheless instructive in view of the preceding discussion. Reduction of the ferric EDTA complex with superoxide anion is accomplished with a rate constant of $2 \times 10^6 M^{-1} s^{-1}$ producing oxygen and the ferrous complex. Reoxidation occurs via a pH independent process with a rate constant of ~ $10^6 M^{-1} s^{-1}$. This pH independence and the magnitude of the rate constant suggest that the reoxidation is accomplished via an inner-sphere binding of superoxide to the coordination site generated by the loss of a bound water (see reaction 10.13 above).

The iron(II) complex of the synthetic porphyrin ligand, tetrakis(4-N-methylpyridyl)porphine has been reported to catalyze this dismutation (82), but mechanistic details are limited owing to the complex's propensity to form oxo bridged dimers and as a consequence lose activity (83). Other Fe-based synthetic SOD catalysts have been reported with amino pyridine ligands such as N,N,N',N'-tetrakis(2-pyridylmethyl)ethylenediamine and tris[N-(2-pyridylmethyl)-2-aminoethyl]amine (84), but mechanistic details are lacking.

Recently, a series of Fe(III) pentaazamacrocyclic ligands were reported to be active SOD catalysts and to exhibit reaction kinetics which reveal that reduction is the rate-limiting process in the catalytic cycle (24). These same macrocyclic ligands were reported to provide highly active SOD catalysts with Mn(II) (see section 4.2.1 above), but with the major difference that the rate-limiting step is oxidation. Thus, the resting state of the catalyst for each metal is the high-spin d^5 complex. These Fe(III) complexes exist in water in the physiological pH regime as the equilibrium mixture of the *trans*-$Fe^{III}(L)(H_2O)(OH)]^{2+}$ and the *trans*-$Fe^{III}(L)(OH)_2]^+$ complexes. From kinetic and mechanistic studies, the authors establish that the aquo, hydroxo complex, *trans*-$Fe^{III}(L)(H_2O)(OH)$ is the active form. The reaction proceeds via a dissociative inner-sphere pathway in which the loss of the axial water ligand from Fe(III) generating a vacant coordination site is the rate-limiting process. Subsequent binding of superoxide anion to Fe(III) provides the pathway for reduction of Fe(III) to Fe(II). This mechanism is analogous to the general mechanism represented by equation 10.9 for an inner-sphere reduction step.

5. Superoxide Dismutase Enzymes

5.1 Copper-zinc superoxide dismutases

5.1.1 Structural characteristics

CuZnSOD is found in the cytosol and extracellular compartments of virtually all eukaryotic cells and in the periplasm of Gram-negative bacteria (1). (One notable exception is a large group of marine arthropods with no CuZnSOD that have a cytosolic MnSOD in its place (85).) Most CuZnSODs are homodimeric proteins, with each of the two equivalent subunits containing a copper and a zinc ion and a molecular weight of approximately 16,000. All of the characterized CuZnSODs are remarkably stable relative to other intracellular proteins. Two monomeric CuZnSODs (from rice (86) and from the periplasmic space of *E. coli* (87)) have also been isolated. With the exception of the CuZnSODs from *E. coli* (88) and *P. leiognathi* (89), the amino acid sequences, protein fold, substrate binding channel, and active site configurations of CuZnSOD have been highly conserved throughout evolution (90).

The metal binding site of CuZnSOD consists of six histidines and an aspartate (91). Three of the histidines (His46, His48, and His120, using yeast or human CuZnSOD numbering) bind exclusively to copper in either the reduced, copper(I)-containing or the oxidized, copper(II)-containing forms of the protein. Two of the histidines (His71 and His80) and the aspartate (Asp 83) bind exclusively to the zinc(II) ion. The imidazole ring of the "bridging histidine", His63, binds exclusively to the zinc ion in reduced CuZnSOD and the copper(I) ion sits in a nearly trigonal plane of three histidines (91, 92). In the oxidized form of the enzyme, the copper ion has changed position, moving closer to His63 and binding to it so that His63 acts as a bridging ligand between the Cu^{2+} and the Zn^{2+} ions (91). A water molecule also enters the first coordination sphere of the copper(II) ion (Figure 1).

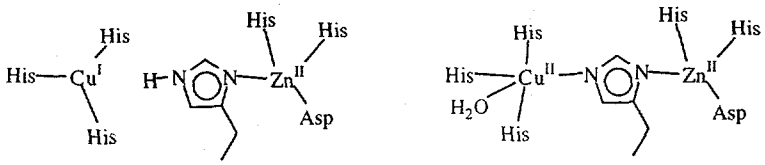

Figure 1. Schematic representation of the metal binding sites in CuZnSOD

Aside from the structural differences in the metal binding region, which consist mainly of a large displacement of the copper ion in reduced versus oxidized CuZnSOD and some small changes in liganding histidines and the water ligand at the copper site, the structures of the oxidized and reduced enzymes are extremely similar. One particularly important structural feature that is virtually identical in both the oxidized and reduced enzymes is the funnel shaped channel that provides access to the copper ion. This channel is 24 Å wide at the surface of the protein but becomes progressively narrower until it is only 4 Å across directly above the copper ion (93-95). This narrowing of the bottom of the channel has the effect of limiting ligand binding to Cu^{2+} in the oxidized form of the enzyme to small anions similar in size and charge to superoxide, e.g., cyanide, azide, and fluoride, and making the enzyme highly specific for reaction with superoxide. One anion that is particularly prevalent *in vivo* that is apparently excluded from approaching the copper(II) center closely is ascorbate anion, whose rate of reaction with the oxidized enzyme is extremely slow despite very favorable redox potentials (96).

5.1.2 What makes CuZnSOD a good SOD?

5.1.2.1 Substrate recognition

A wealth of information strongly supports substrate recognition occurring via electrostatic interactions between O_2^- and either oxidized or reduced CuZnSOD. Superoxide is drawn into and docked in the active site by an electrostatic field created by positively charged amino acid side chains near and in the funnel-like channel that lies directly above the catalytic copper ion. A series of theoretical calculations (97-99) of the electrostatic attraction of the enzyme for O_2^- and experimental determinations (100-102) of the SOD activities of CuZnSODs containing chemical modification or mutagenic substitution of conserved amino acid residues that form the channel have demonstrated the essential role of electrostatic guidance in the enzymatic activity. Recent NMR studies on monomeric mutant CuZnSOD suggest further that changes and/or fluctuations in the channel structure may be important in determining the catalytic efficiency of those enzymes (103-105). On the basis of all of these experiments and calculations, it seems clear that the selectivity of the enzyme for reaction with superoxide and the efficiency of the disproportionation reaction catalyzed by the enzyme depends critically on the ability of the enzyme to maintain the precisely engineered channel undisturbed and that the electrostatic steering of O_2^- into the active site of enzyme is one particularly important feature of CuZnSOD that makes it an efficient biological catalyst of O_2^- disproportionation.

5.1.2.2. The role of Arginine 143

Arg143 is located in the active site channel, approximately 6 Å above the copper(II) ion in the oxidized structure, and it plays an important role in generating the electrostatic field that draws superoxide to the mouth of the active site channel (98, 100). In addition, the positively charged guanidinium group of that residue is well positioned to assist in guiding the superoxide anion down the channel, hydrogen bonding with it as it approaches the copper center in either the oxidized or reduced enzyme. This hydrogen bonding interaction localizes O_2^- directly above the copper ion in a position from which a redox reaction could occur by either an outer or inner sphere electron transfer mechanism (see discussion of possible mechanisms below). Recently the pH dependence of the catalytic rate of wild type single and double mutants of *Xenopus leavis* CuZnSOD was determined using pulse radiolysis (106). The results, which are in agreement with those from site directed mutagenesis experiments on the human enzyme (98), indicated that 25% of the electrostatic steering of superoxide is due to Arg143 and that this residue plays a key role in orienting O_2^- as it approaches the copper ion.

5.1.2.3 Coordination of superoxide and other anions to copper(I) and copper (II)

One particularly important issue is whether the superoxide substrate enters the first coordination sphere of either the copper(II) or copper(I) ions in the oxidized or reduced enzyme, respectively, in the course of the catalytic mechanism. In the case of oxidized CuZnSOD, anions such as azide (N_3^-), cyanide (CN^-), and fluoride (F^-) bind directly to Cu^{2+} in the enzyme, and the latter two ligands have been shown to exchange rapidly. Therefore it is likely that superoxide enters into the first coordination sphere of the Cu^{2+} ion, forming a $Cu^{2+}(O_2^-)$ complex, prior to the electron transfer that forms the products Cu^+ and O_2 (91). For the re-oxidation of reduced CuZnSOD by superoxide, however, the situation is less clear. The trigonal planar $Cu(I)(His)_3$ center seems unlikely to have a high affinity for binding a fourth ligand, based on comparisons with model cuprous complexes. Nevertheless, clear evidence of anion binding to the reduced protein has been obtained by NMR (107).

A recent study of azide binding to both oxidized and reduced CuZnSOD using Fourier transform infrared spectroscopy appears to have resolved this apparent dilemma (108). The antisymmetric stretching band of N_3^- was observed to shift to higher energy upon coordination to oxidized CuZnSOD, consistent with coordination to copper(II). By contrast, interaction of N_3^- with reduced CuZnSOD or with the copper-free enzyme resulted in a band shift to lower energy similar to that observed upon reaction of N_3^- with free lysine or arginine. It was concluded that N_3^- does not directly coordinate to

copper(I) in reduced CuZnSOD but instead binds to the guanidinium group of Arg143. It is likely that superoxide binds in a similar fashion in both cases, i.e., to copper(II) in oxidized CuZnSOD but to Arg143 in reduced CuZnSOD. The implications of this finding for the mechanism are discussed further in section 5.1.3.

5.1.2.4 The role of His63

The imidazole ring of His63 binds solely to Zn^{2+} in the reduced enzyme whereas it is deprotonated to form imidazolate which bridges Cu^{2+} and Zn^{2+} when the enzyme is oxidized. The His63-Zn^{2+} moiety clearly plays an important role in the SOD mechanism since removal of zinc from the enzyme makes the SOD activity pH dependent (109). A similar pH dependent decrease in activity was observed in studies of the site directed mutant His63Ala that lacks the bridging histidine (110). Studies of the SOD activity of the zinc-deficient enzyme by pulse radiolysis established that the reduction of the copper(II) form of the enzyme by superoxide remained fast and pH independent. Therefore it could be concluded that oxidation of the copper(I) form of the enzyme by superoxide had become rate-determining and pH dependent. These observations suggest that the His63-Zn^{2+} moiety plays an important role in determining the rate of the oxidation of reduced CuZnSOD by superoxide and its lack of dependence on pH. It was postulated that the coordination of the His63-Zn^{2+} moiety to copper(II) that creates the imidazolate bridge prevents strong binding of the hydroperoxy anion to copper and thus facilitates rapid loss of the peroxide product.

5.1.2.5 Thermal Stability and pH Independence

CuZnSODs share the characteristic of remarkably high thermal stability relative to other intracellular proteins; irreversible deactivation has an onset of greater than 70 degrees C. Differential scanning calorimetry (DSC) studies of both bovine and human CuZnSOD indicate that unfolding occurs at ca. 80-90 degrees C (111, 112). An enzyme with increased thermal stability was constructed using site directed mutagenesis by replacing Cys6 by Ala and Cys111 by Ser in the human enzyme (113). This thermal stability seems to result in large part from reducing the extent of irreversible unfolding. The copper and zinc ions are known to confer thermal stability to the enzyme as the apoenzyme undergoes denaturation approximately 40 degrees lower than the hohenzyme (114). The rate constant for superoxide dismutation is independent of pH over the pH range of 5-9 while the activity drops at higher pH. A suggestion for this decrease in activity has been electrostatic effects resulting from deprotonation of amino acid resuidue(s) at or near the active site channel (115, 116). The pH independence of the activity is in marked contrast with the pH dependence observed for

small amino acid complexes of copper (see section 4.1). It is thus quite striking that the pH independence of CuZnSOD is lost when zinc is removed from the active site (see section 5.1.3.3).

5.1.3 Mechanism of superoxide disproportionation catalyzed by CuZnSOD

5.1.3.1 Overall reaction

The SOD reaction catalyzed by CuZnSOD occurs by a two step mechanism, just as in the model complexes, with reduction of Cu^{2+} to Cu^{+} by the first O_2^- and re-oxidation of Cu^{+} to Cu^{2+} by a second O_2^-. During the reduction step, the bond between His63 and the copper ion is broken, and one equivalent of H^+ per enzyme subunit is required to protonate the imidazolate ring of His 63. Upon re-oxidation, two equivalents of H^+ are eliminated in the form of H_2O_2 and the Cu^{2+} -His63-Zn^{2+} bridge reforms. Under conditions of saturating superoxide concentrations, there apparently is not time for the imidazolate bridge to break and reform between successive reactions with superoxide, suggesting that the breaking of the bridge in reduced CuZnSOD is not absolutely required prior to reoxidation by superoxide in the catalytic mechanism (117). However such high concentrations of superoxide are unlikely ever to be reached in a cell *in vivo* under normal circumstances.

5.1.3.2 Reduction of oxidized CuZnSOD by superoxide$^-$

Reduction of oxidized CuZnSOD by O_2^- is believed to occur through an inner-sphere electron transfer mechanism, as discussed above in section 5.1.2.3. A likely mechanistic pathway is summarized in Figure 2. In this mechanism, superoxide is drawn into and maneuvered through the funnel-like channel by a positive electrostatic field. Once at the bottom of the funnel, it binds to the Cu^{2+} ion, hydrogen bonds with Arg143, and displaces the water that was bound to the copper ion. X-ray crystal structures of either cyanide (118) or azide (119) bound to copper(II) in CuZnSOD support such a configuration for superoxide if it binds to the copper ion prior to electron transfer. Recent results from Quian *et al.*(120) suggest that protonation of the bridging imidazolate of His63 is very rapid and coupled to the electron transfer, eliminating the interaction between His 63 and copper and thus breaking the Cu^{2+}-Im-Zn^{2+} bridge. Once reduced to Cu^{+}, the copper ion moves 1 Å away from its initial position toward the remaining three histidine ligands, making room for a proton to attach to His 63, and adopting a trigonal planar ligand geometry. In contrast to the copper site, the zinc site appears to remain invariant during the reaction and His63 is

held in place by coordination to Zn^{2+}, ready to reform the imidazolate bridge upon re-oxidation.

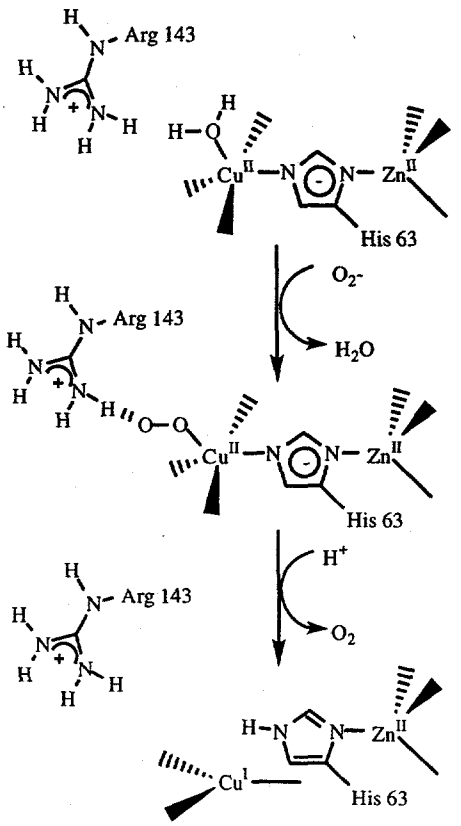

Figure 2. Inner sphere mechanism for reduction of oxidized CuZnSOD by superoxide

5.1.3.3 Oxidation of reduced CuZnSOD by superoxide$^-$

The rate of reaction of superoxide with CuZnSOD is strongly dependent on ionic strength (121), consistent with the dominance of the electrostatic field that attracts superoxide to the metalloenzyme, but is independent of the oxidation state of the copper ion, as evidenced by the identical rate constants for reaction of superoxide with the oxidized and the reduced forms of CuZnSOD, i.e., 2 x 10^9 $M^{-1}s^{-1}$ (91). Thus

superoxide enters the substrate channel in the reduced enzyme just as it did in the case of the oxidized enzyme and presumably docks similarly to Arg143 but without complexing to the copper (see section 5.1.2.3). For superoxide to oxidize the Cu^+ ion, there must be at least one proton intimately associated with the O_2^- as it accepts an electron to become peroxide (see section 2.3). Presumably the proton on His63, which is very close according to the crystal structure (92), plays that role.

If only one proton transfers to the peroxide as it is formed, the product is the hydroperoxide anion, HOO^-. This oxy anion is likely to complex to Cu^{2+}, if it is formed at this point (reaction 10.55).

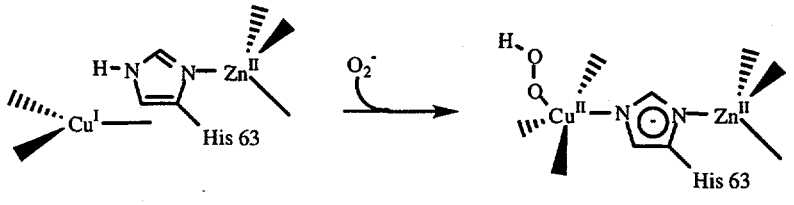

(10.55)

Protonation and loss of hydrogen peroxide would then follow. An alternative possibility is that two protons, one from a water molecule and the other from His63, transfer simultaneously with a through space electron transfer from Cu^+, forming hydrogen peroxide directly. This possibility is described in Figure 3

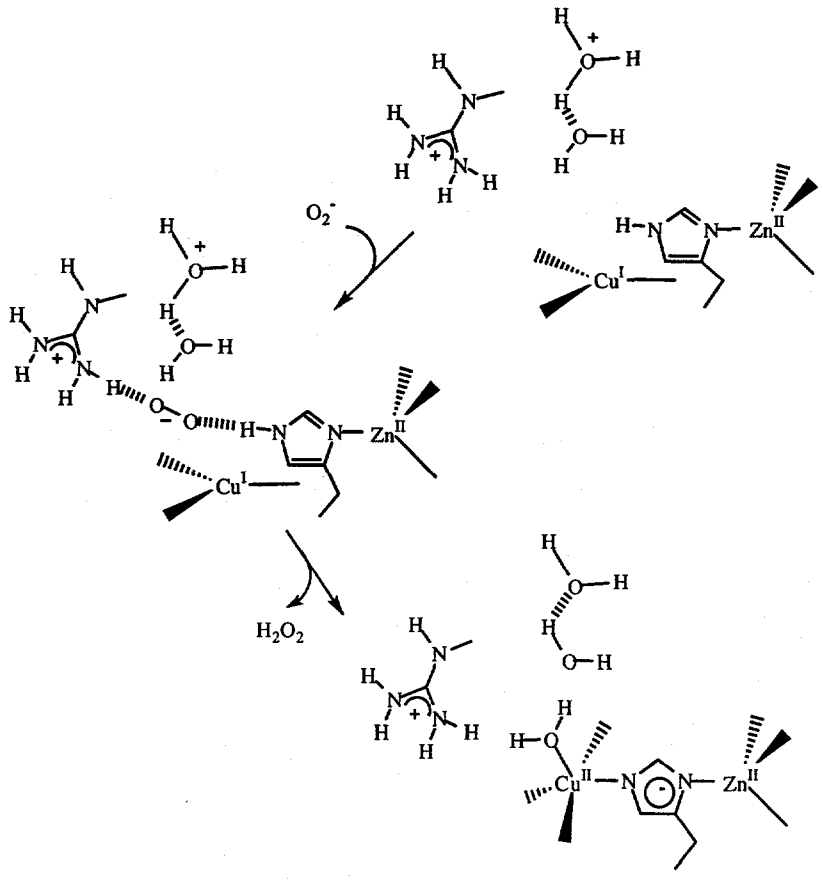

Figure 3. Outer sphere mechanism for oxidation of reduced CuZnSOD by superoxide. A chain of conserved water molecules has been observed in the active site channel in all of the crystal structures (91).

When zinc is removed from the zinc binding site of CuZnSOD, the oxidation of the reduced enzyme by superoxide becomes pH dependent (see section 5.1.2.4 above). One possible explanation is that the strong binding of the zinc-imidazolate moiety to copper(II) in oxidized CuZnSOD weaken the bond to the hydroperoxide anion so that it binds only weakly or not at all (reaction 10.56). In the absence of the zinc-imidazolate ligand on copper(II), the loss of peroxide may be fast only at low pH (109).

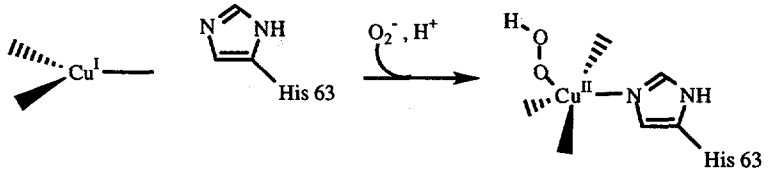

(10.56)

5.2 Manganese superoxide dismutase

5.2.1 Protein structure: active site and substrate access channel

Manganese superoxide dismutase (Mn SOD) occurs with great frequency in both prokaryotic and eukaryotic cells where it exists as monomers, dimers, or tetramers of approximately 26,000 Da subunits. Human mitochondrial MnSOD, for example, is a homotetramer and the *E.coli* enzyme is a homodimer. X-ray crystal structural studies of both oxidized $Mn^{III}SOD$, and reduced $Mn^{II}SOD$ have shown conserved structures and metal binding sites (122-124). Three histidines, one aspartate, and one solvent water molecule bind to the manganese ion in a nearly trigonal bipyramidal geometry.

The MnSOD subunits fold into two domains, N-terminal and C-terminal, which consist mainly of α-helix. The subunits are held together by polar interactions and hydrogen bonds. Within each subunit, four residues, two histidines from the N-terminal domain (His28, His81; numbering according to the *E. coli* enzyme) and a histidine and an aspartate from the C-terminal domain (His171 and Asp167), plus a solvent molecule (water or hydroxide) are bound to the manganese ion forming a trigonal bipyramidal geometry. The metal binding site is further stabilized by a highly conserved extended hydrogen bonding network involving Tyr34 and Gln146, which are hydrogen bonded to the metal binding ligands H_2O and Asp167 (125). This proton linkage network is involved in the binding of the ligands to the metal center as well as in proton transfer, both of which are critical to the efficient turnover of the catalytic reaction.

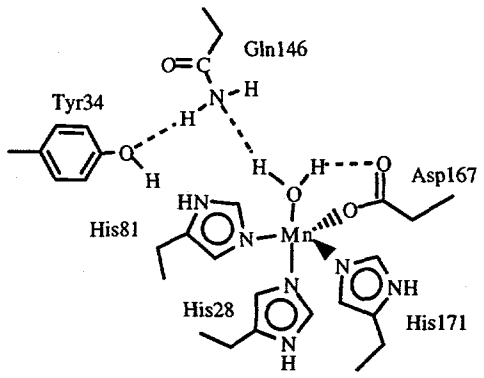

Figure 4. Active site configuration of MnSOD

The pathway from bulk solvent to the manganese ion is a channel lined with residues from both subunits. The residues in the channel, many of which are either conserved or semi-conserved, may electrostatically facilitate entry of the substrate.

5.2.2 Mobile metal center in the anion adduct

Distorted trigonal bipyramid geometry and anion (F^-, N_3^-) binding to the metal center for both the oxidized and reduced forms of the enzyme are indicated from a variety of spectral measurements, including optical absorption, circular dichroism, NMR and EPR (126). While the x-ray crystal structure of the Mn(III)SOD azide complex shows six atoms around the metal center (123), the ligand field optical spectra of Mn(III)SOD are characteristic of five-coordination at room temperature (295 K) with a clean conversion to a six-coordinate geometry at low temperature (127). An X-ray crystal structure of the Mn(III)SOD azide complex revealed that the water ligand was retained and that the largest structural change was the elongation of the metal carboxylate bond from 1.80 Å to 2.25 Å,(123) suggesting that the carboxylate group rather than water may be displaced upon anion binding (see Figure 5). This mobile five-coordinate metal center may serve to facilitate the release of peroxide through rebinding of the displaced ligand to the metal ion, a key kinetic element in the redox catalysis of the enzyme (125, 127).

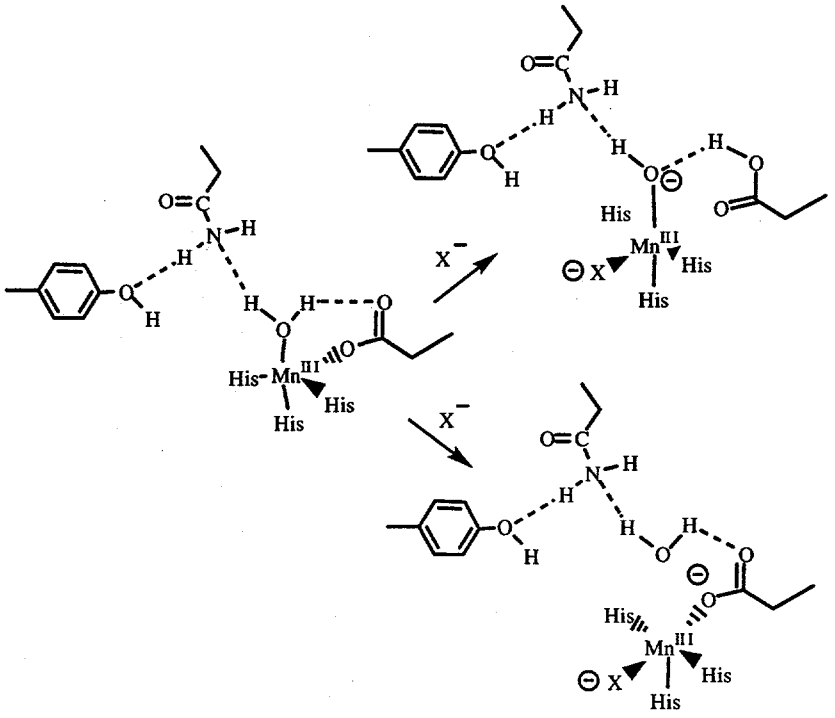

Figure 5. Anion binding to Mn(III)SOD induces dissociation of either the Asp (upper) or water (lower) ligand from the mobile five-coordinate metal center.

5.2.3 MnSOD mechanism

5.2.3.1 Reduction of oxidized enzyme by superoxide

The reduction of Mn(III)SOD to Mn(II)SOD by superoxide and the release of O_2 is fast (ca. $10^9 M^{-1}s^{-1}$). According to the proposed mobile five-coordinate metal center model discussed earlier, superoxide approaches the metal center and binds to the Mn^{3+} ion, and a ligand detaches from the metal ion (see Figure 5). The detached ligand remains in the outer coordination sphere until it rebinds to the Mn^{2+} ion after dioxygen is released.

$$(H_2O)Mn^{3+}SOD \xrightarrow{-H_2O} Mn^{3+}SOD \xrightarrow{O_2^-} (O_2^-)Mn^{3+}SOD \xrightarrow{\text{fast}} Mn^{2+}SOD + O_2 \qquad (10.57)$$

5.2.3.2 Oxidation of the reduced enzyme by superoxide

It has been generally assumed that the oxidation of Mn^{2+}SOD by superoxide occurs by an inner sphere pathway, but recent studies of manganese-containing synthetic SODs suggest that an outer sphere pathway should be considered as well. The mechanism that has been widely assumed for the oxidation of Mn^{2+}SOD to Mn^{3+}SOD by superoxide involves inner sphere electron transfer from the metal ion to the superoxide ligand coupled with proton transfer to the peroxide product as it is formed. In accord with this mechanism is the observation that Mn^{2+}SOD is known to be capable of binding simple anions similar to superoxide. However, FeSOD, which is extremely similar to MnSOD in its structure and many of its other properties, does not bind such anions in its reduced, Fe^{2+}, state (see discussion below). If the SOD mechanism is the same for both MnSOD and FeSOD, then an outer sphere mechanism should be considered for both. Both inner and outer sphere mechanisms for oxidation of Mn^{2+}SOD to Mn^{3+}SOD by superoxide are therefore considered in this section.

Inner sphere electron transfer from Mn^{2+} to superoxide and transfer of a proton to the peroxo group would form a Mn^{3+}-hydroperoxo complex. An additional proton is needed to release H_2O_2 from the Mn^{3+}-hydroperoxo intermediate, reforming the oxidized enzyme. Among these processes, O_2^- binding to Mn^{2+}SOD is believed to be diffusion controlled, and inner-sphere electron transfer within $Mn^{2+}(O_2^-)$ would be expected to be very rapid. Therefore, if this mechanism is correct, the rate determining step is probably release of H_2O_2 from the Mn^{3+}-hydroperoxo intermediate (reaction 10.58).

$$Mn^{2+}SOD + O_2^- \rightarrow (O_2^-)Mn^{2+}SOD \xrightarrow{H^+} (HOO^-)Mn^{3+}SOD \xrightarrow{H^+} Mn^{3+}SOD + H_2O_2 \qquad (10.58)$$

Efficient proton transfer is critical to the release of the peroxo group and regeneration of the active oxidized enzyme. The rate determining step in the overall catalytic reaction therefore will depend on the efficiency of delivery of protons from the enzyme. The protons necessary for oxidation of Mn^{2+}SOD by O_2^- may come from the hydrogen bond network enveloping the metal binding site, involving Tyr34, Gln146 and two metal bound ligands (solvent H_2O and Asp167) (see Figure 6). This mechanism involves both the mobile five-coordinate metal center and the proton network at the active site (see Figure 6). Tyr34 is proposed to play an important role in this proton network by maintaining the appropriate protonation state of the network and the proper coordination state and geometry of the active metal center. Tyr34 is strictly conserved in all Mn and FeSODs. Mutation of Tyr to Phe greatly reduces the activity of MnSOD.(123, 125, 127)

Outer-sphere electron transfer from superoxide to Mn^{2+} through the metal bound H_2O ligand (see Figure 5) would avoid formation of a Mn^{3+}-hydroperoxide. This alternative mechanism looks particularly attractive in light of the recent demonstration

of such a mechanism in some pentaazamacrocyclic complexes of manganese (22) (see section 4.2.1).

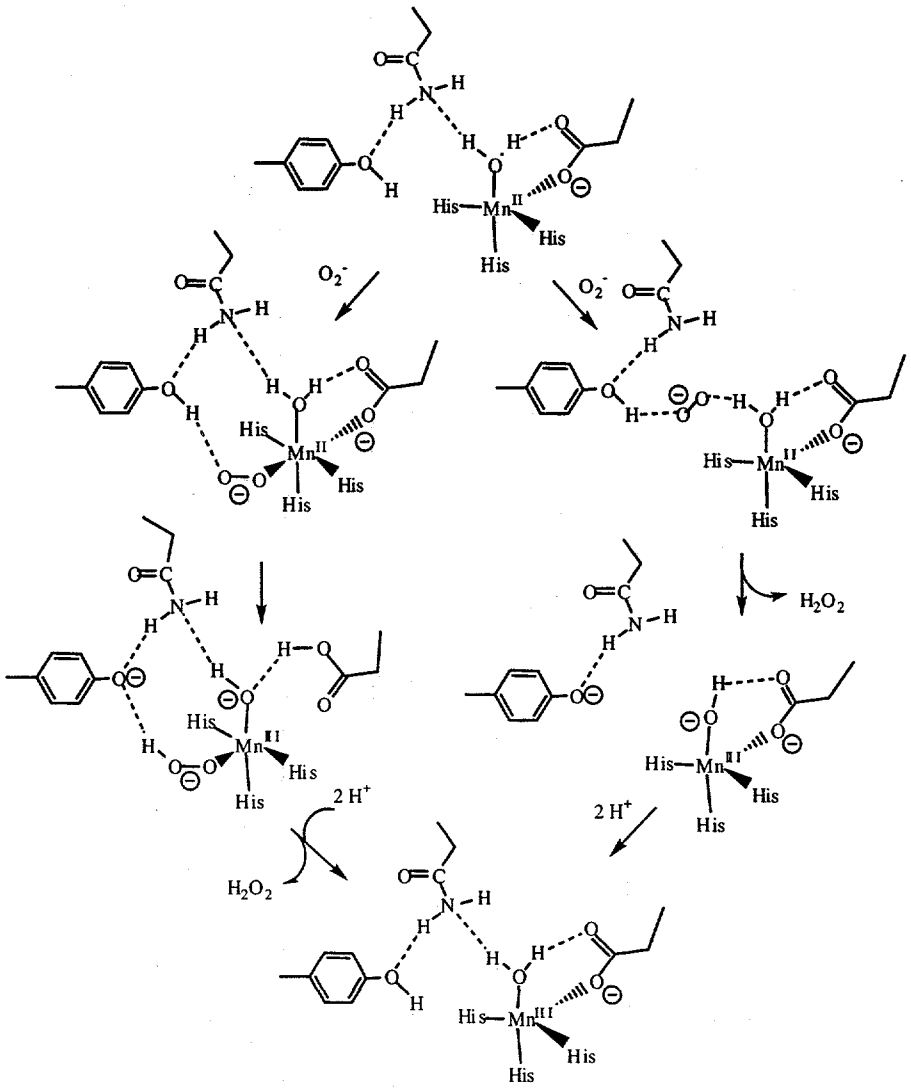

Figure 6. Inner (left) and outer (right) sphere mechanism for oxidation of Mn(II)SOD by superoxide.

5.2.3.4 Inactive form of MnSOD

The disappearance of superoxide radical in the presence of MnSOD is first-order at relatively low superoxide-to-enzyme concentrations while, at sufficiently high concentrations of superoxide-to-enzyme, a multiphase process is observed. This process involves a rapid initial disappearance of some percentage of $O_2^{\cdot}$, followed by a zero-order decay of the substrate and then a final abrupt depletion of the remaining $O_2^{\cdot}$. A mechanism involving conversion of MnSOD to an inactive form is consistent with the observed kinetic behavior, where the zero-order decay represents buildup of the inactive enzyme. Under conditions where the concentration of $O_2^{\cdot}$ is sufficiently low to avoid buildup of the inactive form, catalytic disproportionation of superoxide by the active MnSOD is diffusion controlled ($k \sim 10^9\ M^{-1}s^{-1}$).

Two different mechanisms have been suggested previously for the formation and nature of the inactive form of the enzyme. One mechanism postulates that a conformational change of the metal binding site leads to inactive MnSOD.(128, 129) Another suggestion is that the bound peroxy ligand, O_2^{2-}, isomerizes from an end-on bound peroxy species to a triangular side-on bound peroxy (72, 130). We suggest here a third possibility: If the reoxidation of Mn^{2+}SOD occurs normally by an outer sphere oxidation via coordinated water (see Figure 6), the inactive complex could be one in which a hydroperoxide ligand has entered the first coordination sphere of the Mn^{3+} ion and from which protonation and hydrogen peroxide dissociation occur only slowly. Thus, if proton delivery from amino acid residues or water in the active site to the bound hydroperoxy is not in the proper steric alignment, the proton transfer could be slow giving rise to a less active or inactive form of the enzyme. In this regard, it is interesting to note that the pentaazamacrocyclic complexes of manganese that are SOD mimics release hydrogen peroxide only when they are reduced by superoxide (see reaction 10.44).

Of interest is a recent study (130) of the dismutation mechanism of human MnSOD where isomerizaton from the inhibited form/dissociation of the bound peroxide was reported to be 30 times faster than the corresponding process in *T. thermophilus* MnSOD. It is tempting to speculate that in MnSODs, the entrance of hydroperoxide into the first coordination sphere and subsequent dissociation of peroxide may be processes that are very sensitive to subtle changes in the environment. Whether the enzyme enters into the inactive cycle will depend significantly on the enzyme:substrate ratio.

5.3 Iron superoxide dismutase

5.3.1 Active metal center and metal binding specificity

MnSOD and FeSOD share highly homologous sequences and almost identical protein structure and metal binding sites. However, with a few notable exceptions, the catalytic activity is greatly decreased if Mn is substituted into FeSOD or the reverse. Close examination of the high resolution crystal structures reveal important difference in the hydrogen bond network around the metal centers in these enzymes. The only significant change within 10 Å of the active site of FeSOD occurs at the position corresponding to Glu146 in MnSOD, where histidine or alanine is substituted for the highly conserved glutamine. In FeSOD, the histidine or alanine residue in that position does not interact with Fe bound solvent while in MnSOD, a glutamine residue at this position forms a hydrogen bond with Mn-bound solvent. This rather subtle difference may be critical to the metal selection.(131, 132)

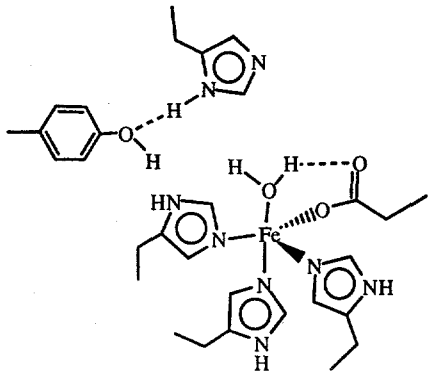

Figure 7. Active site configuration of FeSOD. (Note that some FeSODs have Ala in place of the non-liganding His.)

Although most MnSODs and FeSODs are metal ion specific, some SODs from bacteria such as *P. shermanii, B. thetaiotaomicron and S. mutans,* are active with either Mn or Fe. These SODs have been termed "cambialistic". They can be isolated from cell culture contain either Mn or Fe, or both, depending on the availability of the metal ions in the medium (133-135).

5.3.2 FeSOD mechanism

MnSOD and FeSOD are very similar in many respects, but they differ in one important property that may provide useful insights into the mechanism of reaction of the reduced enzymes with superoxide. Unlike Mn^{2+}SOD, Fe^{2+}SOD does not appear to bind anions in its inner coordination sphere (126) and therefore is unlikely to react by the inner sphere mechanism described in Figure 6. This failure of Fe^{2+}SOD to bind anions combined with the slow rate of dissociation expected for hydroperoxide complexes of Mn^{3+} or Fe^{3+} make the outer sphere pathway in Figure 6 a strong possibility.

5.4 Reactions of SODs with hydrogen peroxide

Reduced CuZnSOD and FeSOD are oxidized slowly by hydrogen peroxide in a Fenton-type reaction and they are inactivated in the process by the hydroxyl radical that is generated at the active site. In the case of reduced CuZnSOD, the reaction goes exclusively via HO_2^- (55, 136). In contrast, MnSOD does not undergo Fenton-type chemistry with hydrogen peroxide. The deleterious effects of OH radical production makes it tempting to speculate that the presence of MnSOD rather than CuZnSOD or FeSOD in mitochondria of most eukaryotic cells may be advantageous since that organelle is likely to produce the highest concentrations of hydrogen peroxide in the cell as a consequence of respiration. The unreactive behavior with peroxide is certainly an essential part of any synthetic SOD that is to be used as a drug and is a property of the pentaazamacrocylic complexes of manganese that are being developed as SOD mimics (23).

6. Conclusion

In this review we have focused much of our discussion on the mechanistic details of how the native enzymes function and how mechanistic developments/insights with synthetic small molecule complexes possessing SOD activity have influenced our understanding of the electron transfer processes involved with the natural enzymes. A few overriding themes have emerged. Clearly, the SOD enzymes operate at near diffusion controlled rates and to achieve such catalytic turnover activity, several important physical principles must be operative. Such fast electron transfer processes requires a role for protons; i.e., proton-coupled electron transfer ("H-atom transfer") solves the dilemma of charge separation developing in the transition state for the electron transfer step. Additionally, outer-sphere electron transfer is likely a most important pathway for manganese and iron dismutases. This situation arises because the ligand exchange rates on these two ions in water never exceed ~10^{+7} s^{-1}; consequently, 10^{+9} catalytic rates require more subtle mechanistic insights. In contrast,

copper complexes can achieve diffusion controlled ($>10^{+9}$) exchange rates in water; thus inner-sphere electron transfer processes are more likely to be operative in the Cu/Zn enzymes.

Recent studies have continued to expand our understanding of the mechanism of action of this most important class of redox active enzymes, the superoxide dismutases, which have been critical in the successful adaptation of life on this planet to an oxygen-based metabolism. The design of SOD mimic drugs, synthetic models compounds that incorporate this superoxide dismutase catalytic activity and are capable of functioning in vivo, offers clear potential benefits in the control of diseases, ranging from the control of neurodegenerative conditions, such as Parkinson's or Alzheimer's disease, to cancer.

This research was carried out at Brookhaven National Laboratory under contract DE-AC02-98CH10886 with the U.S. Department of Energy and supported by its Division of Cheimical Sciences, Office of basic Energy Sciences.

References

1. Fridovich I., *J Biol Chem* **272** (1997), 18515-18517.
2. Scandalios J. G., Ed., *Oxidative stress and the molecular biology of antioxidant defenses* (Cold Spring Harbor Laboratory Press, Plainview, NY, 1997).
3. Valentine J. S., et al., *Curr. Op. Chem. Biol.* (1998), in press.
4. Halliwell B.and Gutteridge J. M. C., *Free radicals in biology and medicine* (Oxford University Press, New York, ed. 2nd, 1989).
5. Keyer K.and Imlay J. A., *Proc Natl Acad Sci USA* **93** (1996), 13635-13640.
6. Aust S. D., *Toxicol Lett* **82** (1995), 941-944.
7. Thomas C. E.and Aust S. D., *Arch Biochem Biophys* **248** (1986), 684-689.
8. Aikens J.and Dix T. A., *Arch Biochem Biophys* **305** (1993), 516-525.
9. Aikens J.and Dix T. A., *J Biol Chem* **266** (1991), 15091-15098.
10. Dix T. A., et al., *Biochemistry* **35** (1996), 4578-4583.
11. Reaume A. G., et al., *Nat Genet* **13** (1996), 43-47.
12. Huang T. T., et al., *Arch Biochem Biophys* **344** (1997), 424-432.
13. Longo V. D., Gralla E. B.and Valentine J. S., *J Biol Chem* **271** (1996), 12275-12280.
14. Li Y., et al., *Nat Genet* **11** (1995), 376-381.
15. Lebovitz R. M., et al., *Proc Natl Acad Sci USA* **93** (1996), 9782-9787.
16. Irani K., et al., *Science* **275** (1997), 1649-1652.
17. Weiss R. H., et al., *J Biol Chem* **271** (1996), 26149-26156.
18. Peretz D., Solomon D., Weinraub D.and Faraggi M., *Int. J. Radiat. Biol.* **42** (1982), 449-456.
19. Batinic-Haberle I., Liochev S. I., Spasojevic I.and Fridovich I., *Arch Biochem Biophys* **343** (1997), 225-233.
20. Weinraub D., Levy P.and Faraggi M., *International J. Radiat. Biol.* **50** (1986), 649.
21. Riley D. P.and Weiss R. H., *J. Am. Chem. Soc.* **116** (1994), 387-388.
22. Riley D. P., Lennon P. J., Neumann W. L.and Weiss R. H., *J. Am. Chem. Soc.* **119** (1997), 6522 -6528.
23. Riley D. P.and Weiss R. H., *Cattech* **1** (1997), 41-49.
24. Zhang D.-L., et al., *Inorg. Chem.* **37** (1998), 956.
25. Pinto A. L., Hellinga H. W.and Caradonna J. P., *Proc Natl Acad Sci USA* **94** (1997), 5562-5567.
26. Afanas'ev I. B., *Superoxide Ion: Chemistry and Biological Implications* (CRC Press Inc., Boca Raton, FL, 1991).
27. Bielski B. H. J.and Cabelli D. E., *Int. J. Radiat. Biol.* **59** (1991), 291.
28. Sawyer D. T., *Oxygen Chemistry* (Oxford University Press, New York, 1991).
29. Bielski B. H. J., *Photochem. Photobiol.* **28** (1978), 645.

30. Bielski B. H. J., Cabelli D. E., Arudi R. L.and Ross A. B., *J. Phys. Chem. Ref. Data* **14** (1985), 1041-1100.
31. Wardman P. J., *Phys. Chem. Ref. Data* **18** (1989), 1637-1755.
32. Stanbury D. M., *Adv. Inorg. Chem.* **33** (1989), 69-138.
33. Rao P. S.and Hayon E., *J. Phys. Chem.* **79** (1975), 392-402.
34. Sawyer D. T.and Valentine J. S., *Acc. Chem. Res.* .
35. Friedman H.and Newton M. J. J., *Electroanal. Chem.* **204** (1986), 21.
36. Hudis J.and Dodson R. W., *J. Am. Chem. Soc.* **78** (1956), 911.
37. Buxton G. V., Greenstock C. L., Helman W. P.and Ross A. B., *J. Phys. Chem. Ref. Data* **17** (1988), 513.
38. Riley D. P., Rivers W. J.and Weiss R. H., *Analyt. Biochemistry* **196** (1991), 344.
39. Klug-Roth D.and Rabani J., *J. Phys. Chem.* **80** (1976), 588.
40. Brigelius R., et al., *Hoppe-Seyler's Z. Physiol. Chem.* **356** (1975), 739.
41. Brigelius R., et al., *FEBS Let.* **47** (1974), 72.
42. Weinstein J.and Bielski B., *J. Am. Chem. Soc.* **102** (1980), 4916.
43. Cabelli D. E., Holcman J.and Bielski B. H. J., *J. Am. Chem. Soc.* **109** (1987), 3665.
44. Graham D. R., Marshall L. E., Reich K. A.and Sigman D. A., *J. Am. Chem. Soc.* **102** (1980), 5419.
45. Que B. G., Downey K. M.and So A. G., *Biochemistry* **19** (1980), 5987.
46. Marshall L. E., Graham D. R., Reich K. A.and Sigman D. A., *Biochemistry* **20** (1981), 244.
47. Goldstein S.and Czapski G., in *Superoxide and Superoxide Dismutase in Chemistry, Biology and Medicine* Rotilio G., Ed. (Elsevier Scientific Peb., New York, 1985) pp. 64-66.
48. Goldstein S.and Czapski G., *J. Am. Chem. Soc.* **105** (1983), 7276.
49. Rabani J., Klug-Roth D.and Lilie J., *J. Phys. Chem.* **77** (1973), 1169-1175.
50. Bjergebakke E., Sehested K.and Rasmussen O. L., *Radiat. Res.* (1976), 433-442.
51. Kozlov Y. N.and Berdnikov V. M., *Russ. J. Phys. Chem.* **47** (1973), 338-340.
52. Tait A. M., Hoffman M. Z.and Hayon E., *Inorg. Chem.* **15** (1976), 934-939.
53. Goldstein S.and Czapski G., *Inorg. Chem.* **24** (1985), 1087-1092.
54. Goldstein S.and Czapski G., *J. Am. Chem. Soc.* **105** (1983), 7276-7280.
55. Cabelli D. E., Allen D., Bielski B. H.and Holcman J., *Journal of Biological Chemistry* **264** (1989), 9967-9971.
56. Baral S., Lume-Pereira C., Janata E.and Henglein A., *J. Phys. Chem.* **90** (1996), 6025.
57. Cabelli D. E.and Bielski B. H. J., *J. Phys. Chem.* **88** (1984), 3111.

58. Cabelli D. E.and Bielski B. H. J., *J. Phys. Chem.* **88** (1984), 6291.
59. Koppenol W. H., et al., *Arch. Biochem. Biophys.* (1986), 251.
60. Pick-Kaplan M.and Rabani J., *J. Phys. Chem.* **80** (1976), 1840.
61. Lati J.and Meyerstein D., *J. Chem. Soc. Dalton* (1978), 1105.
62. Stein J., et al., *Inorg. Chem.* **18** (1979), 3511.
63. Rush J. D.and Maskos Z., *Inorg. Chem.* **29** (1990), 897.
64. Jacobsen F., Holcman J.and Sehested K., *J. Phys. Chem. A* **101** (1997), 1324-1328.
65. Cabelli D. E., in *Photochemistry and Radiation Chemistry: Complementary Methods for Electron Transfer Studies* Wishart J. F.andNocera D. G., Eds. (American Chemical Society, Washington D.C.,).
66. Faulkner K. M., Stevens R. D.and Fridovich I., *Arch. Biochem. Biophys.* **310** (1994), 341-346.
67. Darr D., Zarilla K. A.and Fridovich I., *Arch. Biochem. Biophys.* **258** (1987), 351-355.
68. Rush J. D., Maskos Z.and Koppenol W. H., *Arch. Biochem. Biophys.* **289** (1991), 97-102.
69. Gray B.and Carmichael A. J., *Biochem. J.* **281**795-802.
70. Baudry M., et al., **192** (1993), 964-968.
71. Goetz F.and Lengfelder E., in *Oxy-Radicals and their Scavenger Systems, Molecular Aspects* Cohen G.andGreenwald R. A., Eds. (Elsevier Biomedical, New York, 1983), vol. 1, pp. 228-233.
72. Bull C., Niederhoffer E. C., Yoshida T.and J.A. F., *J. Am. Chem. Soc.* **113** (1991), 4069-4076.
73. Hoganson C. W.and Babcock G. T., *Science* **277** (1997), 1953-1956.
74. Caudle M. T.and Pecoraro V. L., *J. Am. Chem. Soc.* **119** (1997), 3415.
75. Barb W. G., Baxendale J. H., George P.and Hargrave K. R., *Trans. Faraday Soc.* **47** (1951), 462.
76. Barb W. G., Baxendale J. H., George P.and Hargrave K. R., *Trans. Faraday Soc.* **47** (1951), 591.
77. Rush J. D.and Bielski B. H. J., *J. Phys. Chem.* **89** (1985), 5062.
78. Jayson G. G., Parsons B. J.and Swallow A. J., *J. Chem. Soc. Faraday Trans. I* **68** (1972), 2053.
79. Jayson G. G., Parsons B. J.and Swallow A. J., *J. Chem. Soc. Faraday Trans. I* **69** (1972), 1079.
80. Jayson G. G., Parsons B. J.and Swallow A. J., *J. Chem. Soc. Faraday Trans. I* **69** (1973), 236.
81. Bull C., McClune G.and Fee J. A., *J. Am. Chem. Soc.* **105** (1983), 5290.
82. Pasternack R. F.and Halliwell B., **101** (1979), 1026.
83. Weiss R. H., et al., *J. Biol. Chem.* **268** (1993), 23049.

84. Nagano T., Hirano T.and Hirobe M., *J. Biol. Chem.* **264** (1989), 9243.
85. Brouwer M., et al., *Biochemistry* **36** (1997), 13381 -13388.
86. Kanematsu S.and Asada K., *Plant Cell Physiol.* **30** (1989), 381-391.
87. Battistoni A.and Rotilio G., *Febs Lett* **374** (1995), 199-202.
88. Pesce A., et al., *Journal Of Molecular Biology* **274** (1997), 408-420.
89. Bourne Y., et al., *Proceedings Of the National Academy Of Sciences Of the United States Of America* **93** (1996), 12774-12779.
90. Bordo D., Djinovic K.and Bolognesi M., *Journal Of Molecular Biology* **238** (1994), 366-386.
91. Bertini I., Mangar S.and Viezzoli M. S., *Adv. Inorg. Chem.* **45** (1998), 127 - 250.
92. Ogihara N. L., et al., *Biochemistry* **35** (1996), 2316-2321.
93. Tainer J. A., et al., *J. Mol. Biol.* **160** (1982), 181-217.
94. Getzoff E. D., et al., *Nature* **306** (1983), 287-290.
95. Tainer J. A., Getzoff E. D., Richardson J. S.and Richardson D. C., *Nature* (1983), 284-.
96. Lyons T. J., et al., *Proceedings Of the National Academy Of Sciences Of the United States Of America* **93** (1996), 12240-12244.
97. Sines J. J., Allison S. A.and McCammon J. A., *Biochemistry* **29** (1990), 9403-9412.
98. Fisher C. L., et al., *Proteins-Structure Function and Genetics* **19** (1994), 24-34.
99. Desideri, *J. Mol. Biol* **233** (1992), 337-342.
100. Beyer W. F., Jr., Fridovich I., Mullenbach G. T.and Hallewell R., *J Biol Chem* **262** (1987), 11182-11187.
101. Cocco D., et al., *FEBS Lett* **150** (1982), 303-306.
102. Getzoff E. D., et al., *Nature* **358** (1992), 347-351.
103. Banci L., et al., *Magnetic Resonance In Chemistry* **35** (1997), 845-853.
104. Banci L., et al., *European Journal Of Biochemistry* **234** (1995), 855-860.
105. Banci L., et al., *Journal Of Biological Inorganic Chemistry* **2** (1997), 295-301.
106. Polticelli F., et al., *Protein Science* **5** (1996), 248-253.
107. Mota de Freitas D., Ming L. J., Ramasamy R.and Valentine J. S., *Inorganic Chemistry* **29** (1990), 3512-3518.
108. Leone M., et al., *Biochemistry* **37** (1998), 4459-4464.
109. Ellerby L. M., Cabelli D. E., Graden J. A.and Valentine J. S., *Journal Of the American Chemical Society* **118** (1996), 6556-6561.
110. Graden J. A., Ellerby L. M., Roe J. A.and Valentine J. S., *Journal Of the American Chemical Society* **116** (1994), 9743-9744.
111. Roe J. A., et al., *Biochemistry* **27** (1988), 950-958.
112. Lepock J. R., et al., *Arch. BIochem. Biophys.* **241** (1985), 243-251.

113. McRee D. E. R., S. M., et al., *J. Biol. Chem.* **265** (1990), 14234-14241.
114. Lepock J. R., Frey H. E.and Hallewell R. A., *J. Biol. Chem.* **265** (1990), 21612-21618.
115. Banci L., Bertini I., Luchinat C.and Viezolli M. S., *Inorg. Chem.* **32** (1993), 1403.
116. Polticelli F., et al., *Arch. Biochem. Biophys.* **321** (1995), 123-128.
117. Fee J. A.and Bull C., *Journal of Biological Chemistry* **261** (1986), 13000-13005.
118. Djinovic-Carugo K., et al., *FEBS Lett* **349** (1994), 93-98.
119. Djinovic-Carugo K., et al., *Journal Of Molecular Biology* **240** (1994), 179-183.
120. Qian W., Luo Q. H.and Shen M. C., *Bioelectrochem. Bioenergetics* **39** (1996), 291-294.
121. Argese E., et al., *Biochemistry* **26** (1987), 3224-3228.
122. Ludwig M. L., Metzger A. L., Pattridge K. A.and Stallings W. C., *J Mol Biol* **219** (1991), 335-358.
123. Lah M. S., et al., *Biochemistry* **34** (1995), 1646-1660.
124. Stallings W. C., et al., *Free Radic Res Commun* **12** (1991), 259-268.
125. Whittaker M. M.and Whittaker J. W., *Biochemistry* **36** (1997), 8923-8931.
126. Whittaker J. W.and Whittaker M. M., *J. Am. Chem. Soc.* **113** (1991), 5528-5540.
127. Whittaker M. M.and Whittaker J. W., *Biochemistry* **35** (1996), 6762-6770.
128. Pick M., Rabani J., Yost F.and Fridovich I., *J. Am. Chem. Soc.* **96** (1974), 7329-7333.
129. McAdam M. E., Fox R. A., Lavelle F.and Fielden E. M., *Biochem. J.* **165** (1977), 71-79; 81-87.
130. Hsu J. L., et al., *J Biol Chem* **271** (1996), 17687-17691.
131. Lim J. H., et al., *J Mol Biol* **270** (1997), 259-274.
132. Cooper J. B., et al., *J Mol Biol* **246** (1995), 531-544.
133. Sehn A. P.and Meier B., *Biochem J* **304** (1994), 803-808.
134. Meier B., et al., *Biochem J* **310** (1995), 945-950.
135. Matsumoto T., et al., *Biochemistry* **30** (1991), 3210-3216.
136. Fuchs H. J. R.and Borders C. L., Jr., *Biochem. Biophys. Res. Comm.* **116** (1983), 1107-1113.